

Measurement of the neutron capture cross section of the fissile isotope ^{235}U with the CERN n_TOF total absorption calorimeter and a fission tagging based on micromegas detectors

J. Balibrea-Correa⁴, E. Mendoza⁴, D. Cano-Ott⁴, M. Kr̩ička⁶, S. Altstadt¹, J. Andrzejewski², L. Audouin³, V. Béc̩ares⁴, M. Barbagallo⁵, F. Beč̩v̩ř⁶, F. Belloni⁷, E. Berthoumieux⁷, J. Billowes⁸, V. Boccone, D. Bosnar⁹, M. Brugger¹⁰, F. Calviño¹¹, M. Calviani¹⁰, C. Carrapiço¹², F. Cerutti¹⁰, E. Chiaveri^{10,7}, M. Chin¹⁰, N. Colonna⁵, G. Cortés¹¹, M.A. Cortés-Giraldo¹³, M. Diakaki¹⁴, C. Domingo-Pardo¹⁵, R. Dressler¹⁶, I. Durán¹⁷, C. Eleftheriadis¹⁸, A. Ferrari¹⁰, K. Fraval⁷, V. Furman¹⁹, K. Göbel¹, C. Guerrero¹⁰, M.B. Gómez-Hornillos¹¹, S. Ganesan²⁰, A.R. García⁴, G. Giubrone¹⁵, I.F. Gonçalves¹², E. González⁴, A. Goverdovski²¹, E. Griesmayer²², F. Gunsing⁷, T. Heftrich¹, S. Heintz¹⁶, A. Hernández-Prieto^{10,11}, J. Heyse²³, D.G. Jenkins²⁴, E. Jericha²², F. Käppeler²⁵, Y. Kadi¹⁰, D. Karadimos¹⁴, T. Katabuchi²⁶, V. Ketlerov²¹, V. Khryachkov²¹, N. Kivel¹⁶, P. Koehler²⁷, M. Kokkoris¹⁴, J. Kroll⁶, C. Lampoudis⁷, C. Langer¹, E. Leal-Cidoncha¹⁷, C. Lederer²⁸, H. Leeb²², L.S. Leong³, J. Lerendegui-Marco¹³, M. Licata^{29,30}, R. Losito¹⁰, A. Mallick²⁰, A. Manousos¹⁸, J. Marganiec², T. Martínez⁴, C. Massimi^{29,30}, P. Mastinu³¹, M. Mastromarco⁵, A. Mengoni³², P.M. Milazzo³³, F. Mingrone²⁹, M. Mirena³⁴, W. Mondelaers²³, C. Paradela¹⁷, A. Pavlik²⁸, J. Perkowski², A.J.M. Plompen²³, J. Praena¹³, J.M. Quesada¹³, T. Rauscher³⁵, R. Reifarh¹, A. Riego-Perez¹¹, M. Robles¹⁷, C. Rubbia¹⁰, J.A. Ryan⁸, M. Sabaté-Gilarte^{10,13}, R. Sarmiento¹², A. Saxena²⁰, P. Schillebeeckx²³, S. Schmidt¹, D. Schumann¹⁶, P. Sedyshev¹⁹, G. Tagliente⁵, J.L. Tain¹⁵, A. Tarifeño-Saldivia¹⁵, D. Tarrío¹⁷, L. Tassan-Got³, A. Tsinganis¹⁰, S. Valenta⁶, G. Vannini^{29,30}, V. Variale⁵, P. Vaz¹², A. Ventura²⁹, M.J. Vermeulen²⁴, V. Vlachoudis¹⁰, R. Vlastou¹⁴, A. Wallner³⁶, T. Ware⁸, M. Weigand¹, C. Weiss²², T. Wright⁸, P. Žugec⁹, and the n_TOF Collaboration

¹ Goethe University Frankfurt, Germany

² University of Lodz, Poland

³ Institut de Physique Nucléaire, CNRS-IN2P3, Univ. Paris-Sud, Université Paris-Saclay, 91406 Orsay Cedex, France

⁴ Centro de Investigaciones Energeticas Medioambientales y Tecnológicas (CIEMAT), Spain

⁵ Istituto Nazionale di Fisica Nucleare, Sezione di Bari, Italy

⁶ Charles University, Prague, Czech Republic

⁷ CEA Saclay, Irfu, Gif-sur-Yvette, France

⁸ University of Manchester, UK

⁹ University of Zagreb, Croatia

¹⁰ European Organization for Nuclear Research (CERN), Switzerland

¹¹ Universitat Politècnica de Catalunya, Spain

¹² Instituto Superior Técnico, Lisbon, Portugal

¹³ Universidad de Sevilla, Spain

¹⁴ National Technical University of Athens, Greece

¹⁵ Instituto de Física Corpuscular, Universidad de Valencia, Spain

¹⁶ Paul Scherrer Institut (PSI), Villingen, Switzerland

¹⁷ University of Santiago de Compostela, Spain

¹⁸ Aristotle University of Thessaloniki, Thessaloniki, Greece

¹⁹ Joint Institute for Nuclear Research (JINR), Dubna, Russia

²⁰ Bhabha Atomic Research Centre (BARC), India

²¹ Institute of Physics and Power Engineering (IPPE), Obninsk, Russia

²² Technische Universität Wien, Austria

²³ European Commission, Joint Research Centre, Geel, Retieseweg 111, 2440 Geel, Belgium

²⁴ University of York, UK

²⁵ Karlsruhe Institute of Technology, Campus North, IKP, 76021 Karlsruhe, Germany

²⁶ Tokyo Institute of Technology, Japan

²⁷ Oak Ridge National Laboratory (ORNL), Oak Ridge, TN 37831, USA

²⁸ University of Vienna, Faculty of Physics, Vienna, Austria

²⁹ Istituto Nazionale di Fisica Nucleare, Sezione di Bologna, Italy

³⁰ Dipartimento di Fisica e Astronomia, Università di Bologna, Italy

³¹ Istituto Nazionale di Fisica Nucleare, Sezione di Legnaro, Italy

³² Agenzia nazionale per le nuove tecnologie (ENEA), Bologna, Italy

³³ Istituto Nazionale di Fisica Nucleare, Sezione di Trieste, Italy

³⁴ Horia Hulubei National Institute of Physics and Nuclear Engineering, Romania

³⁵ Department of Physics, University of Basel, Switzerland

³⁶ Australian National University, Canberra, Australia

Abstract. The accuracy on neutron capture cross section of fissile isotopes must be improved for the design of future nuclear systems such as Gen-IV reactors and Accelerator Driven Systems. The High Priority Request List of the Nuclear Energy Agency, which lists the most important nuclear data requirements, includes also the neutron capture cross sections of fissile isotopes such as $^{233,235}\text{U}$ and $^{239,241}\text{Pu}$.

A specific experimental setup has been used at the CERN n_TOF facility for the measurement of the neutron capture cross section of ^{235}U by a set of micromegas fission detectors placed inside a segmented BaF₂ Total Absorption Calorimeter.

1. Introduction

The neutron capture cross sections of fissile isotopes play an essential role for the understanding of the actual critical nuclear systems and the development of future systems such as Gen-IV reactors and Accelerator Driven Systems [1]. The actual nuclear data required is summarized in the High Priority Request List of the Nuclear Energy Agency [2]. The measurement of the neutron capture cross section in such isotopes is difficult due to the dominant γ -ray background produced in the competing neutron-induced fission reactions.

A specific experimental setup [3] has been used in the horizontal beam line at the CERN n_TOF neutron time-of-flight (TOF) facility [4,5] to tackle this problem. The concept of the technique was proven in 2010 in a test experiment [3] and the real measurement on ^{235}U was performed in 2012. The aim of this paper is to describe the experimental setup, the data analysis carried out and the results obtained in the neutron energy range from 0.2 to 20 eV.

2. Experimental setup

The setup consists of a set of Fission Tagging Micromegas (FTMG) [6] detectors placed inside the segmented n_TOF Total Absorption Calorimeter (TAC) [7].

During the experiment, ten isotopically enriched samples of $^{235}\text{U}_3\text{O}_8$ (41.1 ± 0.1 mg) with thickness $7.6 \cdot 10^{-7}$ At/barns were used. The samples were manufactured at the Joint Research Center-Geel [8]. The ^{235}U targets were grouped in a stack of eight samples and other two encapsulated inside two FTMG detectors. A second configuration with ten FTMG detectors, one per ^{235}U target, was used to cross check the neutron capture data obtained at low neutron energies. The first configuration was preferred in the measurement for the better signal to background ratio. The ensemble was placed inside a sealed fission chamber filled with a gas mixture of 88% Ar, 10% CF₄ and 2% isobutane at 1 atm for the operation of the FTMG detectors. The fission chamber was located in the center of the TAC surrounded by a 5 cm thick borated polyethylene neutron absorber in order to reduce the amount of scattered neutrons detected by the TAC. The capture and the neutron-induced fission reactions on ^{235}U targets were simultaneously measured by the TAC and the FTMG detectors as a function of TOF.

3. Experimental yield determination

The neutron-induced fission and capture yields are experimentally determined as a function of the neutron

energy as

$$Y_{n,x}(E_n) = \frac{C_{tot,x}(E_n) - C_{bkg,x}(E_n)}{\varepsilon_x(E_n) \cdot \phi(E_n)} \quad (1)$$

where $C_{tot,x}(E_n)$ and $C_{bkg,x}(E_n)$ are the total and the background counts registered by the TAC ($x = \gamma$) or by the FTMG detectors ($x = f$), $\varepsilon_x(E_n)$ is the corresponding detection efficiency, and $\phi(E_n)$ the neutron fluence.

For the TAC, many background components have to be subtracted: (i) the background related to the material that intercepts the beam; (ii) the activity of the BaF₂ crystals, ambient background and sample activity; (iii) the prompt-fission γ background; (iv) and the background induced by the prompt-fission neutrons. The background due to the interaction of the neutron beam with the ^{235}U targets, i.e., due to elastic scattering and delayed β -decay of the fission fragments, was negligible.

Dedicated measurements with the same experimental configuration, including all dead material layers without the ^{235}U targets, were performed in order to estimate the components (i) and (ii). Component (iii) is obtained accurately via the coincident events between the FTMG and TAC (C_{tagg}), by selecting the events with high γ -ray multiplicity which correspond only to (n,f) reactions [3,9]. This background component is calculated as C_{tagg}/ε_f , where ε_f is the fission detection efficiency. The background component (iv) was calculated by Monte Carlo simulations.

In the FTMG detectors, the energy thresholds were chosen to remove the α -particles from the sample activity, thus neglecting the background in these detectors.

The shape of the neutron fluence has been verified by the ratio between the $^{235}\text{U}(n,f)$ cross section obtained from the FTMG detectors and ENDF/B-VII.1 obtaining differences within the 2% in the neutron range of interest.

4. Normalization

The normalization of the neutron capture cross section has been performed to the accurately known integral ^{235}U fission cross section in the neutron energy range from $E_1 = 7.0$ to $E_2 = 11.0$ eV, $\int_{E_1}^{E_2} \sigma_f(E) dE = (246 \pm 1)$ barns·eV, using the ratio of capture and neutron-induced fission yields. The neutron capture cross section integral is obtained in the thin target approximation as

$$\int_{E_1}^{E_2} \sigma_\gamma(E) dE = \int_{E_1}^{E_2} \sigma_f(E) dE \frac{\int_{E_1}^{E_2} \frac{C_{tot,\gamma}(E) - C_{bkg,\gamma}(E)}{\varepsilon_\gamma(E) \cdot \phi(E)} dE}{\frac{1}{\varepsilon_f} \int_{E_1}^{E_2} \frac{C_{tot,f}(E)}{\phi(E)} dE} \quad (2)$$

where, $\sigma_\gamma(E)$, and $\sigma_f(E)$ are the capture and neutron-induced fission cross sections, respectively, and assuming that ε_f does not depend on the neutron energy.

In this approximation, the normalization depends neither on the mass of the samples nor on the absolute value of the neutron intensity or the beam area covered by the ^{235}U targets, thus reducing the systematic uncertainties. Thereby, the accuracy of the normalization depends only on the statistics achieved and the determination of the efficiency for the capture and fission events.

4.1. Fission detection efficiency

The fission detection efficiency ε_f , defined as the probability to detect a neutron-induced fission reaction in any of the ten ^{235}U samples with the FTMG detectors, was experimentally obtained from the ratio of the number coincidences between the FTMG detectors and the TAC to the total number of neutron-induced fission reactions detected by the TAC. This ratio is the detection efficiency of the FTMG detectors under the assumption that the probability of detecting a fission reaction in the FTMG detectors does not depend on its detection in the TAC. The number of neutron-induced fissions in the TAC was calculated taking into account only events with total deposited energies (E_{sum}) larger than the neutron separation energy of ^{236}U , $S_n(^{236}\text{U}) = 6.55$ MeV, thereby excluding the $^{235}\text{U}(n,\gamma)$ reactions. The background contribution in such conditions was obtained from the dedicated background measurements. The fission detection efficiency was calculated in different ^{235}U resonances under different conditions on E_{sum} and crystal multiplicity (m_{cr}), finding compatible results.

The value obtained was $\varepsilon_f = 0.1847 \pm 0.0022$, where the uncertainty includes both the statistical and systematic uncertainties. We have verified experimentally that ε_f is constant in the neutron energy range of interest.

4.2. TAC detection efficiency for $^{235}\text{U}(n,\gamma)$ events

The TAC efficiency for neutron capture events has been accurately calculated by means of Monte Carlo simulations following the methodology described in [10,11]. The $^{235}\text{U}(n,\gamma)$ cascades were generated using the DICEBOX code [12] and simulated in the TAC+FTMG geometry with a C++ application [13] based on the GEANT4 toolkit [14,15]. The excellent agreement between the Monte Carlo simulations and the experimental data shown in Fig. 1 permit the TAC efficiency determination with an accuracy of 1%.

5. Results

The $^{235}\text{U}(n,\gamma)$ reaction rate is extracted by conditions on m_{cr} and E_{sum} , which maximize the signal to background ratio without compromising the statistics. The best results were obtained for $2 < m_{cr} < 6$ and $2.5 < E_{sum}(\text{MeV}) < 7.0$. Dead time corrections have been applied following a procedure similar to the methodology described in [16].

The ratio of the experimental resonance integrals to the evaluated values from the ENDF/B-VII.1 and the latest CIELO release (ib18o23g6cnu5ef1) are shown in Fig. 2 and Fig. 3. The evaluated libraries were accurately broadened, processing the resonance parameters with

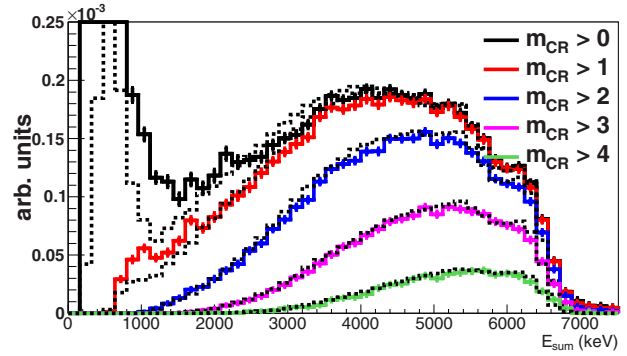


Figure 1. Experimental $^{235}\text{U}(n,\gamma)$ signature detected in the TAC for different m_{cr} cuts compared with Monte Carlo simulations. The Monte Carlo simulations are plotted as dotted lines.

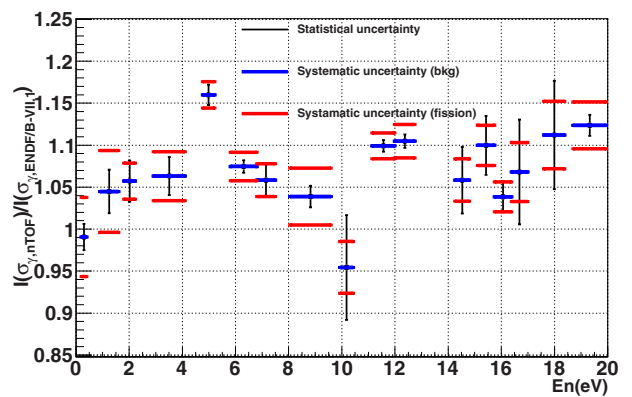


Figure 2. Ratio between the $^{235}\text{U}(n,\gamma)$ cross section measured at the CERN n_TOF facility and the ENDF/B-VII.1 library in the ^{235}U resonances from 0.2 eV to 20 eV.

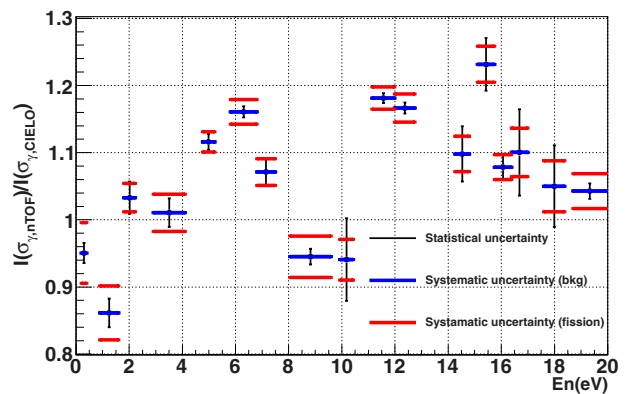


Figure 3. Ratio between the $^{235}\text{U}(n,\gamma)$ cross section measured at the CERN n_TOF facility and the latest CIELO release in the ^{235}U resonances from 0.2 eV to 20 eV.

SAMMY8 code [17] and the experimental resolution. The black line represents the statistical uncertainty and the blue and the red lines represent the systematic uncertainties due to the subtraction of the beam and the prompt-fission background components, respectively. Other sources of systematic uncertainty were neglected in this neutron energy range.

The n_TOF neutron capture data is, on average, $\sim 6\%$ larger than the ENDF/B-VII.1 evaluation in this neutron

energy range. Larger discrepancies are observed with the CIELO evaluation as shown in Fig. 3. However, taking into account all the uncertainties, the n_TOF data are still compatible with both libraries.

6. Summary and conclusions

The ^{235}U neutron capture cross section has been measured at the n_TOF facility relative to the well known ^{235}U neutron-induced fission cross section. The two critical parameters for the normalization have been determined: (i) the TAC detection efficiency for $^{235}\text{U}(n,\gamma)$ events and (ii) the fission detection efficiency.

Our capture cross section data is, on average, $\sim 6\%$ larger than the ENDF/B-VII.1 evaluation in the neutron energy range from 0.2 to 20 eV. Larger discrepancies are observed with the latest CIELO library. The main sources of systematic uncertainties have been carefully determined: (i) the systematic effects associated with the fission γ -ray cascades; (ii) the beam background, and (iii) the dead time corrections. In the investigated neutron energy range component (i) is important.

The ^{235}U neutron capture cross section has been made available to the CIELO project and will be sent soon to EXFOR.

This work was supported in part by the Spanish national company for radioactive waste management ENRESA, through the CIEMAT-ENRESA agreements on 'Transmutación de residuos radiactivos de alta actividad' the Spanish Plan Nacional de I+D+i de Física de Partículas (project FPA2014-53290-C2-1) and the CHANDA project of the 7 th Framework Programme.

References

- [1] A.J. Knoning et al. "CANDIDE: Nuclear data for sustainable nuclear energy" (2009)
- [2] Nuclear Energy Agency "Nuclear Data High Priority Request List " Available at <http://www.oecd-nea.org/dbdata/hprl/hprlview.pl?ID=430>
- [3] C. Guerrero et al. Eur. Phys. J.A **48**, 29 (2012)
- [4] C. Guerrero et al. Eur. Phys. J.A **49**, 27 (2013)
- [5] F. Mingrone et al. EPJ Web of Conferences **122**, 05001 (2016)
- [6] S. Andriamonje et al. J. of Korean Phys. Soc. **59**, 1597–1600 (2011)
- [7] C. Guerrero et al. Nucl. Inst. Meth. A **608**, 424–433 (2009)
- [8] Joint Research Center <https://ec.europa.eu/jrc/en>
- [9] M. Jandel et al. Phys. Rev. Lett. **109**, 202506 (2012)
- [10] C. Guerrero et al. Phys. Rev. C **85**, 044616 (2012)
- [11] E. Mendoza et al. Phys. Rev. C **90**, 034608 (2014)
- [12] F. Bečvář Nuc. Inst. and Meth. A **417**, 434–449 (1998)
- [13] C. Guerrero et al. Nuc. Inst. and Meth. A **671**, 108–117 (2012)
- [14] S. Agostinelli et al. Nucl. Inst. and Meth. A **506**, 250–303 (2003)
- [15] J. Allison et al. Nucl. Inst. and Meth. A **835**, 186–225 (2016)
- [16] E. Mendoza et al. Nucl. Inst. and Meth. A **768**, 55–61 (2014)
- [17] N.M. Larson, Oak Ridge National Laboratory, Oak Ridge, TN, Report No. ORNL/TM-9179/R7, 2006